HYBRID ANTIBACTERIAL MICROFIBERS OF CELLULOSE ACETATE MODIFIED WITH NOVEL PYRIDINE COMPLEXES TO OVERCOME ANTIMICROBIAL RESISTANCE

RUKEN ESRA DEMIRDOGEN

Department of Chemistry, Faculty of Science, Çankırı Karatekin University, TR 18100, Çankırı, Turkey
✉ *Corresponding author: sustainabletechnologiesgroup@gmail.com*

Received January 30, 2022

This study targeted at providing a solution to overcome antimicrobial resistance through new pyridine complexes represented with the general formula $[ML_2Cl_2]$ (L^1: 2-amino-3-methylpyridine; L2: 2,6-diaminopyridine; M: Ni(II), Cu(II), Co(II)). The structures of the synthesized complexes were characterized via FT-IR, ^{1}H-NMR and ^{13}C-NMR techniques. These complexes were used for obtaining hybrid microfibers via electrospinning of cellulose acetate modified with them. The microfibers were characterized via FT-IR spectroscopy and their FE-SEM micrographs were used to study their morphologies and determine their diameters. Thermal properties of the fibers were investigated by a TG/DTA combined system. The antibacterial properties of the complexes and fibers were investigated against representative gram-positive and gram-negative bacterial strains by disc diffusion and broth microdilution tests, as well as by the JIS L 1902: 2008 testing method for antibacterial activity of textiles. The complexes and the hybrid microfibers were observed to have considerable antibacterial activity.

Keywords: pyridine complexes, electrospinning, antimicrobial resistance, antibacterial textile

INTRODUCTION

The causal link discovered between diseases and pathogens has shaped modern medicine. Lately, antimicrobial resistance (AMR) – an important health threat worldwide[1] – has been suspected to play a role in raising the COVID-19 death toll.[2] In the light of the biopsies made on those who have lost their lives due to COVID-19, a secondary bacterial infection that resembled the situation encountered for other viral infections was observed.[3-7] A common symptom of the severe viral respiratory infection is the weakened immune system and exposure of the respiratory system to other pathogens. During severe outbreaks, such as SARS[8,9] and COVID-19, many more of the hospitalized patients were observed to be infected with resistant bacteria (*i.e.*, *Staphylococcus aureus* (SA) and methicillin resistant SA (MRSA)), which in turn increased the mortality rate. Studies showed that, besides the axillae, groin and gastrointestinal tract, SA colonizes ~20% of the individuals persistently through the nasal pathway.

Colonization increases the risk for other post-infection health problems, as it acts as a reservoir for the bacteria to invade the host when the immune response is compromised or when the defense is breached by shaving, surgery, aspiration or insertion of an indwelling catheter, as is the case in intubation.[10,11] Moreover, colonization opens the way for SA to be transmitted to other people. Hence, the great burden put on the Italian and Spanish health systems that caused them to fail during COVID-19 pandemic was caused by AMR-related problems.[12]

Extensive use of first-line traditional antibiotics led to the great global problem of antibiotic/drug resistance to various pathogenic bacteria (gram-negative and gram-positive), which has become a major cause of mortality. Moreover, the increased use of prophylactic antibiotics to prevent secondary bacterial infections that the patients may acquire during their hospitalization, which was the case in COVID-19, [5,6,12,13] caused the emergence of resistant bacteria.[14] Therefore, the fight against AMR requires collective global actions.[1]

In the effort to overcome AMR, the use of antimicrobial drugs, such as iodine, silver and copper,[15,16] offers a potent, effective and eco-friendly alternative for treatment.[17] In order to prevent hospital-acquired diseases, all the devices, apparatus and the textile products used should be hygienic, as these materials, which are in direct contact with the skin, offer an appropriate medium for bacterial

growth under appropriate humidity and temperature conditions.[18]

The quest for obtaining more effective means to fight the diseases caused by pathogens necessitated the development of new antibacterial textiles.[19] Recent antimicrobial aspects of sustainable materials with antimicrobial performance with regard to their potential applications in the biomedical field has brought functional biopolymers and biocompatible polymers to the forefront.[20]

It has been reported that potent antimicrobial, antibacterial and antiviral agents could be obtained from bioactive pyridine derivatives with appropriate N- and O- electron donors, hydroxypyridines, aminopyridines and picolinic acid (pyridine-2-carboxylic acid) that induce apoptosis and immune system responses.[21] The facile processing, eco-friendliness and favorable physical, chemical and biological properties of biopolymers chemically modified to contain biologically active groups and/or by embedding bioactive agents to obtain hybrid materials have rendered them favorable matrices.[23,23] Cellulose has attracted a lot of interest in the development of polymeric biocides obtained by the chemical bonding of antimicrobial active groups on insoluble polymers, as it is one of the most common plant-based organic compounds and it can be recovered and reused for a longer period of time.[24] A semi-synthetic derivative of cellulose – cellulose acetate (CA) – with its acetate functionality coming from the well-known antimicrobial *N,O* containing acetal links, as it down-regulates important global virulence regulators both against gram-negative bacteria (*i.e*., *Pseudomonas aeruginosa* and *Escherichia coli*) and gram-positive bacteria (*i.e*., *Staphylococcus aureus* and *Streptococcus pyogenes*), is widely used for the preparation of semi-permeable, microporous and pH sensitive membranes.[25,26]

Gram-positive and gram-negative bacteria, which are classified according to whether or not bacteria have a *peptidoglycan* wall – a mesh-like layer of sugars and amino acids –, pose unique threats, especially to hospitalized patients with compromised immune systems. While gram-positive bacteria are the reason for serious health problems, gram-negative bacteria are well-known to develop resistance and thus are classified by the Contagious Diseases Center (CDC) as a more serious problem.

Gram-positive bacteria, which are the species that have a peptidoglycan outer layer, are easier to kill since their thick peptidoglycan layer absorbs antibiotics, antimicrobial agents and cleaning products easily. Therefore, effective agents against these species must be able to breach their thick peptidoglycan layer, as well as penetrate the many layers of the gram-negative bacteria, which have a thin peptidoglycan layer. However, gram-negative bacteria, with their additional membrane, can sequester or even remove foreign materials, which include those that are toxic to its insides, such as antibacterial agents, in the space between the membranes (periplasmic space) before they reach the cell itself. Hence, gram-negative bacteria are not easy to destroy. On the other hand, although both gram-positive and negative bacteria survive and even multiply for a long time on dry surfaces, gram-negative bacteria survive for a shorter time. The worst issue is that they can cause drug resistance and especially gram-negative bacteria are more intrinsically resistant to drugs/antibiotics. Gram-positive and gram negative bacteria have different levels of resistance to antibacterial agents, cleansing products and different reactions to dry surfaces. Although new and very expensive antibiotics have been developed to combat these resistant species, there are multiple drug-resistant species that nothing can kill. As a result, only certain antibacterial agents, which can kill both gram-positive and gram-negative bacteria, are approved to be effective and hence health authorities (*i.e*., Environmental Protection Agency (EPA) and World Health Organizarion (WHO)), and new technologies addressing both types of bacteria are constantly sought.

In the quest to develop such effective antibacterial agents and to provide a solution to overcome the ever-existing problem of drug resistance of bacteria, pyridine derivatives, which have appropriate N- and/or O-electron donor groups (*i.e*., hydroxypyridines, aminopyridines and picolinic acid (pyridine-2-carboxylic acid)) and are well-known bioactive compounds with antiviral, antifungal and antibacterial activities that act by inducing apoptosis and immune system responses, have attracted much attention.[27] Hence, in this work, new pyridine derivatives, where the central metal ion binds to the atoms of the donor ligands – such as O, N and S – via strong and selective coordination chemistry[28,29] and the donor ligands that the metal ions would prefer are influenced by the atomic structure, were synthesized and used to obtain antibacterial textiles.

Among pyridine derivatives, amino pyridines have found wide applications in pharmacology and medicine.[30-32] In our previous studies, we had shown that bis(2-fluoropyridine)dichloronickel(II), bis(2-fluoropyridine)dichlorocobalt(II) and bis(2-fluoropyridine)dichlorocopper(II) complexes have

strong antibacterial activity.[33]

The donor ligands preferred determine the selective binding of the proteins to the correct metal that would provide the proper folding or function of the protein.[34] Hence, for the divalent transition metal ions of the fourth period, the preferred binding proceeded in the order Mn(II) < Fe(II) < Co(II)< Ni(II) < Cu(II) > Zn(II).[35] On the other hand, if the metal homeostasis is compromised or when the proteins bind less competitive metal ions at the upper end of this Irving–Williams series, this order is not followed and hence these proteins do not bind to the correct metal cofactor.

Embedding metal ions into appropriate hosts, such as biodegradable and biocompatible polymers, to obtain engineered abiotic surfaces has provided many functional antimicrobial materials (*i.e.* antibacterial textiles, household utensils and medical devices) that kill microorganisms via "contact killing" in a very short period of time ranging from minutes to hours.[36,37] Although the biochemistry that underlies this is not clear, yet, loss of bacterial cell viability has been attributed to uptake of metals such as Cu,[38] Ni[39] and Co,[40] and increased ROS production,[41] which is thought to cause lipid peroxidation,[42] loss of membrane integrity and cell death,[38,41] and surface killing through metal ion mediation, such as Cu-mediation.[41,42] On the other hand, the genetic materials (*i.e.*, plasmid, genomic DNA) released from dead cells are slowly degraded in a manner that depends on the content of the metal ion. Hence, this can prevent lateral gene transfer and thus the spread of the antibiotic resistance genes,[41] especially beneficial for hospital settings.

Among the many different processing methods and techniques proposed for producing polymer fibers, electrospinning has been reported to be the most efficient and cost effective one due to the huge surface area-to-volume ratio, besides the fact that antimicrobial functionalities can be implemented to the polymers both before and after the process.

However, to the best of our knowledge, so far no study on antibacterial cellulose fibers modified with bis(2-amino-3-methylpyridine)dichlorometal (II) and bis(2,6-diaminopyridine)dichlorometal (II) complexes has been reported. In this respect, in the present work, bis(2-amino-3-methylpyridine)dichloronickel (II), $[NiL^1{}_2Cl_2]$, bis(2-amino-3-methylpyridine)dichlorocopper (II), $[CuL^1{}_2Cl_2]$, bis(2-amino-3-methylpyridine)dichlorocobalt (II), $[CoL^1{}_2Cl_2]$, bis(2,6-diaminopyridine)dichloronickel (II) $[NiL^2{}_2Cl_2]$, bis(2,6-diaminopyridine)dichlorocopper (II) $[CuL^2{}_2Cl_2]$ and bis(2,6-diaminopyridine)dichlorocobalt (II) $[CoL^2{}_2Cl_2]$ were synthesized via wet chemistry and their structures were elucidated via FT-IR and ^{1}H-NMR techniques. The morphologies and the diameters of the fibers were examined via SEM. The thermal properties of the complexes and the CA fibers modified with these complexes were studied via a TG/DTA combined system under N_2 atmosphere. Antibacterial studies of the complexes and fibers were carried out against gram-negative (*Escherichia coli* and *Klebsiella pneumonia*) and gram-positive (methicillin-resistant *Staphylococcus aureus* and *Enterococcus faecalis*) bacteria by using disc diffusion and broth microdilution tests, as well as by the JIS L 1902: testing method for antibacterial activity of textiles.

EXPERIMENTAL

Materials and methods

Cellulose acetate (CA) (MW approx. 30.000) and 2-amino-3-methylpyridineand 2,6-diaminopyridine were procured from Sigma-Aldrich. Acetone, dichloromethane (DCM), methanol (MeOH), ethanol (EtOH), Tween-20, $CuCl_2.2H_2O$, $CoCl_2.6H_2O$ and $NiCl_2.6H_2O$ were obtained from Merck. All of the reagents were of analytical grade and were used as received, without further purification. Extended spectrum beta-lactamase (ESBL) producing gram-negative *Escherichia coli* (ATCC 35218) and *Klebsiella pneumoniae* (ATCC 700603), and gram-positive methicillin-resistant *Staphylococcus aureus* (MRSA) (clinical isolate) and *Enterococcus faecalis* (ATCC 29212) were used for antimicrobial studies.

The FT-IR spectra were obtained on a Perkin Elmer Frontier FT-IR spectrometer in the range from 4000 to 400 cm^{-1} using KBr pellets. The ^{1}H-NMR spectra were recorded on a 600 MHz, Agilent Premium Compact spectrometer. TMS (tetramethylsilane) was used as internal reference and D-DMSO as solvent. Field emission scanning electron microscopy (FE-SEM) images were acquired via a Zeiss/Supra 55 FE-SEM. The samples were coated with platinum before FE-SEM measurements. Thermogravimetric (TG) and differential thermal analysis (DTA) curves were recorded simultaneously using a Seiko II TG/DTA 7200 Thermal Analyzer. The samples, with varying mass from 5 to 10 mg, were placed in a platinum crucible and were heated in the temperature range of 25-1000 °C, at a heating rate of 10 °C/min under flowing nitrogen (100 mL/min). The reference material was α-Al_2O_3. Temperature calibration was made by using the melting points of indium and tin obtained from Seiko.

Synthesis of complexes

The [ML_2Cl_2] complexes were synthesized according to the method given in the literature.[43,44] Briefly, 0.025 moles of metal chlorides ($NiCl_2$/$CuCl_2$/$CoCl_2$) were dissolved in 40 mL of EtOH. Then, the ethanolic solutions of 2-amino-3-methylpyridine and 2,6-diaminopyridine prepared by dissolving 0.05 moles of the reagents in 20 mL EtOH were added to the metal chloride solutions. The mixtures were stirred under reflux for 2 hours at a constant temperature of 70 °C. Then, the complexes were precipitated by cooling the solutions to room temperature. Following this, the precipitates were filtered, washed with EtOH and were dried in a desiccator. The open structures of the prepared complexes are given in Figure 1.

Bis(2-amino-3-methylpyridine)dichloronickel(II), [$NiL^1{}_2Cl_2$], FT-IR (KBr, ν_{max}, cm^{-1}): 3332-3585 (N–H stretching vibration), 3201 (aromatic C–H stretching vibration), 2931-2859 (aliphatic C–H stretching vibration), 1651-1570 (aromatic C=C, C=N stretching vibration), 1455-1384 (C–H in-plane bending), 812 (C–H out-of-plane bending), 672-654 (C–C in-plane bending). ^{1}H-NMR (D-DMSO, ppm): 7.74 (4H, N-H), 8.04-6.50 (6H, Ar-H), 3.01-2.50 (6H, Al-H). ^{13}C-NMR (D-DMSO, ppm): 99.66-160.89 (10C, Ar-C), 18.78 (2C, -CH_3).

Bis(2-amino-3-methylpyridine)dichlorocopper(II), [$CuL^1{}_2Cl_2$], FT-IR (KBr, ν_{max}, cm^{-1}): 3446-336 (N–H stretching vibration), 3201 (aromatic C–H stretching vibration), 2930-2871 (aliphatic C–H stretching vibration), 1655-1581 (aromatic C=C, C=N stretching vibration), 1478-1385 (C–H in-plane bending), 847 (C–H out-of-plane bending), 710-593 (C–C in-plane bending).

Bis(2-amino-3-methylpyridine)dichlorocobalt(II), [$CoL^1{}_2Cl_2$], FT-IR (KBr, ν_{max}, cm^{-1}): 3550-3439 (N–H stretching vibration), 3138-3037 (aromatic C–H stretching vibration), 2934-2881 (aliphatic C–H stretching vibration), 1630-1568 (aromatic C=C, C=N stretching vibration), 1474-1400 (C–H in-plane bending), 836 (C–H out-of-plane bending), 700-653 (C–C in-plane bending). ^{1}H-NMR (D-DMSO, ppm): 7.64 (4H, N-H), 8.06-6.52 (6H, Ar–H), 3.01-2.52 (Al-H, 6H). ^{13}C-NMR (D-DMSO, ppm): 99.66-160.89 (Ar-C, 10C), 13.51 (-CH_3, 2C).

Bis(2,6-diaminopyridine)dichloronickel(II), [$NiL^2{}_2Cl_2$], FT-IR (KBr, ν_{max}, cm^{-1}): 3585-3316 (N–H stretching vibration), 3186 (aromatic C–H stretching vibration), 1645-1557 (aromatic C=C, C=N stretching vibration), 1456-1385 (C–H in-plane bending), 785 (C–H out-of-plane bending), 785-653 (C–C in-plane bending).^{1}H-NMR (D-DMSO, ppm): 8.12-7.99 (8H, N-H), 7.05-5.10 (6H, Ar–H). ^{13}C-NMR (D-DMSO, ppm): 99.42-163.38 (10C, Ar-C).

Bis(2,6-diaminopyridine)dichlorocopper(II), [$CuL^2{}_2Cl_2$], FT-IR (KBr, ν_{max}, cm^{-1}): 3551-3301 (N–H stretching vibration), 3182 (aromatic C–H stretching vibration), 1648-1518 (aromatic C=C, C=N stretching vibration), 1466-1386 (C–H in-plane bending), 824 (C–H out-of-plane bending), 703-661 (C–C in-plane bending).

Bis(2,6-diaminopyridine)dichlorocobalt(II), [$CoL^2{}_2Cl_2$], FT-IR (KBr, ν_{max}, cm^{-1}): 3557-3320 (N–H stretching vibration), 3201 (aromatic C–H stretching vibration), 1646-1588 (aromatic C=C, C=N stretching vibration), 1456-1385 (C–H in-plane bending), 807 (C–H out-of-plane bending), 781-600 (C–C in-plane bending). ^{1}H-NMR (D-DMSO, ppm): 8.12-7.99 (8H, N-H), 7.09-5.13 (6H, Ar–H).^{13}C-NMR (D-DMSO, ppm): 99.41-163.36 (10C, Ar-C).

Preparation of cellulose acetate/[ML_2Cl_2] gels

Cellulose acetate (CA)/[ML_2Cl_2] gels were prepared by dissolving 6 g CA in 50 mL acetone under constant stirring at room temperature. Then, 0.1 g of the complexes was added to the solution and stirring was continued for 1 h.

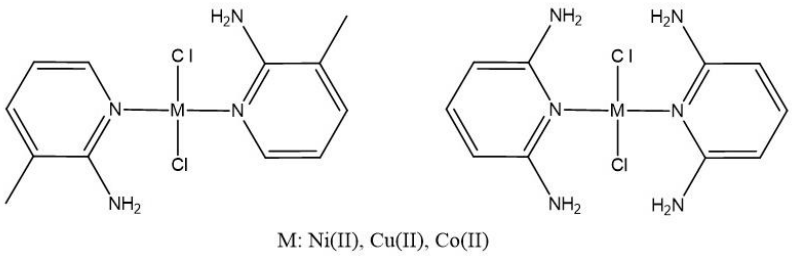

M: Ni(II), Cu(II), Co(II)

Figure 1: Structures of the synthesized complexes

Preparation of cellulose acetate/[ML_2Cl_2] hybrid fibers via electrospinning

Cellulose acetate/[ML_2Cl_2] hybrid fibers were obtained via the electrospinning technique, at a nozzle to

collector distance of 10 cm, at an applied voltage of 12 kV and flow rate of 1.50 mL/min.

Antibacterial activity studies

The complexes and the hybrid microfibers obtained were investigated for their antibacterial activities against four different bacterial strains, namely extended spectrum beta-lactamase (ESBL) gram-negative *Escherichia coli* (ATCC 35218) and *Klebsiella pneumoniae* (ATCC 700603), and gram-positive methicillin-resistant *Staphylococcus aureus* (MRSA) (clinical isolate) and *Enterococcus faecalis* (ATCC 29212). All bacteria were incubated in nutrient broth at 37 °C for 24 h. Prior to testing the antibacterial activity of the materials, the bacteria were inoculated on nutrient agar plates and were incubated at 37 °C for 24 h.

Disc diffusion test

The disc diffusion test reported by the Clinical and Laboratory Standards Institute (CLSI-2012a) was used for comparing the antibacterial activity of the complexes. The bacterial colonies reproduced on the nutrient agar were removed and were placed in Mueller-Hinton broth (Merck) and their turbidity was adjusted, so that bacterial suspensions of McFarland 0.5 (~$1.5x10^8$ cfb/mL) were obtained. These bacterial suspensions were spread on 0.1 mL of Mueller-Hinton Agar (MHA-Merck) surface with sterile forceps. Onto them were added the solutions of the complexes prepared by dissolving them in dimethyl sulfoxide (DMSO) to a concentration of 25 $mg.mL^{-1}$ and sterilized by filtering. 40 µL of this solution was absorbed on the empty discs and the discs were dried at 30 °C. Then, the discs, onto which bacteria were seeded, were placed on Mueller-Hinton agar with sterile pincers. Gentamicin (10 µg/disc, Bioanalyse) discs were used as reference antibiotic and 5% DMSO was used negative control. The media were incubated at 37 °C for 24 hours. Then, the inhibition zones >7 mm were recorded. Analysis was performed in triplicates, and the mean and standard deviation were calculated.

Minimum inhibitory concentration test (MIC)

The broth microdilution method reported by the Clinical and Laboratory Standards Institute (CLSI-2012b) was used to determine the minimum inhibitory concentration of the complexes on bacteria and to confirm the disc diffusion test results. Into all the wells on a 96-well microplate, 100 µL of cation adjusted Mueller-Hinton Broth (BBL) was placed. All the active agents – the complexes – were dissolved in DMSO, so as to have a concentration of 2.5 $mg.mL^{-1}$, and were sterilized by filtering. The active agent solutions were prepared by two-fold serial dilution in the plate wells to obtain the concentration in the range from 0.195 to 1.25 $mg.mL^{-1}$. Then, 100 µL of each complex solution was added to the first row of wells. Each sample was tested three times. Then, 10 µL of bacterial suspensions of $5.0x10^6$ cfu/mL was added to each well. For each bacterium, one well without active agent was used as growth control, and one well with Mueller-Hinton broth and active agent was used to control sterility. Gentamicin (40 $\mu g.mL^{-1}$, Sigma) was used as reference antibiotic. The number of bacteria in the wells was determined by inoculation into 0.1 mL of nutrient agar by diluting the reproduction control wells at a 1:1000 (v/v) ratio. The microplates were incubated at 37 °C for 20-24 h. After incubation, for the dilution wells, which were not turbid, the minimum inhibitory concentration (MIC) was determined. The analysis was performed in triplicates.

Antimicrobial tests of microfibers

The antibacterial activity of the microfibers containing the active agents – the complexes – was determined by the Antibacterial Activity Test Method for Fabrics of the Japanese Institute of Standards (JIS L 1902:2002). All microfibers were sterilized via UV radiation in a biosafety cabinet. 0.4 g of the sterilized microfiber was used as the negative control and the CA microfibers containing the complexes were placed in sterile tubes containing equal amounts of active agents – the complexes. 200 µL of bacterial suspensions, which were adjusted to ~$1x10^5$ cfb/mL, were transferred into each test tube containing hybrid microfiber, the negative control and the antibacterial textile, and were allowed to stay in contact during incubation at 37 °C for 18 h. After incubation, 10 mL of the sterile neutralization solution with a composition of 0.9% NaCl and 0.2% Tween 20 was added to each tube and was gently shaken. Then, 1 mL of solution was taken from each test tube and 3 serial dilutes were made in the test tubes containing nutrient broth and 100 µL solutions taken from each dilution tube were inoculated on nutrient agar, and they were incubated at 37 °C for 24 h. For each sample, 3 parallel assays were performed. At the end of the incubation, the average number of bacteria (log) was determined for each hybrid microfiber. The antibacterial activity of the hybrid microfibers was determined according to the below given formula, as given in the test method:[25]

Decrease in microbial reproduction (Log cfb 24 h) =
log cfb (negative control 24 h) - log cfb (sample 24 h) (1)

$$\% \text{ efficacy} = (\text{cfu/mL at 0 h} - \text{cfu/mL at 24 h}) / (\text{cfu/mL at 0 h}) * 100 \quad (2)$$

The antibacterial activity was considered to be “null or no activity” when the logarithmic decrease in reproduction was <0.5, “moderate” when it was in the range of 0.5-1.0 and “high” when >1.0.[45]

Statistical analysis

The data obtained in the disc diffusion test were analyzed via Minitab 16 (Minitab Inc. State College, PA) package program, using one-way variance analysis (ANOVA). The difference between the groups were determined according to $p < 0.05$ importance level.

RESULTS AND DISCUSSION

Structural characterization

The FT-IR spectra of the complexes were taken in the range of 4000-400 cm^{-1}. The peaks observed in the range 3332-3585 cm^{-1} were attributed to the symmetric and asymmetric stretching modes of NH_2 groups in the complexes. The internal deformation vibrations known as NH_2 scissoring frequency were observed at 1650, 1656, 1630, 1645, 1648 and 1646 cm^{-1} for $[NiL^1{}_2Cl_2]$, $[CuL^1{}_2Cl_2]$, $[CoL^1{}_2Cl_2]$, $[NiL^2{}_2Cl_2]$, $[CuL^2{}_2Cl_2]$ and $[CoL^2{}_2Cl_2]$, respectively. The hetero aromatic C–H (Ar-C-H) stretching vibrations normally occur at 3100-3000 cm^{-1}.[46-49] The synthesized complexes are di-substituted aromatic systems. The peaks at 3138-3201 cm^{-1} were attributed to the aromatic C-H stretching vibrations. For the $[CuL^1{}_2Cl_2]$ complex, the aromatic C-H stretching vibrations were observed to overlap with the symmetric and asymmetric stretching modes of the $-NH_2$ groups. The peaks in the ranges 2931-2859 cm^{-1}, 2930-2871 cm^{-1} and 2934-2881 cm^{-1} indicate the aliphatic asymmetric and symmetric C-H stretching vibrations of $[NiL^1{}_2Cl_2]$, $[CuL^1{}_2Cl_2]$, and $[CoL^1{}_2Cl_2]$ complexes. For these complexes, the peaks observed at 1455-1384 cm^{-1}, 1478-1385 $cm^{-1}$and 1474-1400 cm^{-1} indicate in-plane deformations, whereas the rocking vibrations of the complexes were observed around 1043-998 cm^{-1}, 1042-986 cm^{-1} and 1053-987 cm^{-1}, respectively. The selected important IR bands are given in Table 1.

In the FT-IR spectra of the hybrid CA fibers, the -OH, -C=O and the $-CH_3$ groups were observed at 3476 cm^{-1}, 1736 cm^{-1}, 2924-2872 cm^{-1}, respectively. The FT-IR spectra of the CA/$[ML_2Cl_2]$ hybrid fibers are similar to that of the unmodified CA fibers. The υ(C-C) (1685cm^{-1}) and υ(C-N) (1625cm^{-1}) bands observed in the FT-IR spectra of the pyridine derivative complexes overlap with the vibrations of the CA microfibers.

The ^{1}H-NMR spectra of the complexes – except for the paramagnetic Cu(II) complexes – were obtained in d6-DMSO. The multiplet peaks observed in the range 8.04-6.50 ppm of the $[NiCl_2(L^1)_2]$ and $[CoCl_2(L^1)_2]$ complexes indicate the Ar-H peaks (Ar-H, 6H) in the pyridine ring. The peaks observed at 7.74-7.64 ppm were the N-H peaks (N-H, 4H) in the $-NH_2$ groups in the pyridine ring. The peaks at 3.01-2.50 ppm were attributed to the $-CH_3$ groups. The peaks at 8.12-7.99 ppm of the $[NiCl_2(L^2)_2]$ and $[CoCl_2(L^2)_2]$ complexes were indicative of the $–NH_2$ groups in the pyridine ring (-N-H, 8H) and the multiple peaks at 7.09-5.13 ppm were attributed to the Ar-H (Ar-H, 6H).

The ^{13}C-NMR spectra of the complexes – except for the paramagnetic Cu(II) complexes – were obtained in d6-DMSO. For the $[NiCl_2(L^1)_2]$ and $[CoCl_2(L^1)_2]$ complexes, the peaks observed at 18.78 and 13.51 ppm indicate the carbon in the methyl group ($-CH_3$, 2C). The peaks in the range 99.66-160.89 ppm were attributed to the aromatic carbons in the pyridine ring (Ar -C, 10C). The peaks observed in the range 99.41-163.36 ppm for the $[NiCl_2(L^2)_2]$ and $[CoCl_2(L^2)_2]$ complexes indicate the aromatic carbon atoms (Ar-C, 10C).

Table 1
Selected IR bands

Compound	υ(N-H) (cm^{-1})	υ(Ar-C-H) (cm^{-1})	υ(Al-C-H) (cm^{-1})	υ(Ar–C=C/C=N) (cm^{-1})	δ(C–H) In-plane bending	δ(C–H) Out-of-plane bending	δ(C–C) In-plane bending
$[NiL^1{}_2Cl_2]$	3332-3585	3201	2931-2859	1651-1570	1455-1384	812	672-654
$[CuL^1{}_2Cl_2]$	3446-3360	3201	2930-2871	1655-1581	1478-1385	847	710-593
$[CoL^1{}_2Cl_2]$	3550-3439	3138-3037	2934-2881	1630-1568	1474-1400	836	700-653
$[NiL^2{}_2Cl_2]$	3585-3316	3186	-	1645-1557	1456-1385	785	785-653
$[CuL^2{}_2Cl_2]$	3551-3301	3182	-	1648-1518	1466-1386	824	703-661
$[CoL^2{}_2Cl_2]$	3557-3320	3201	-	1646-1588	1456-1385	807	781-600

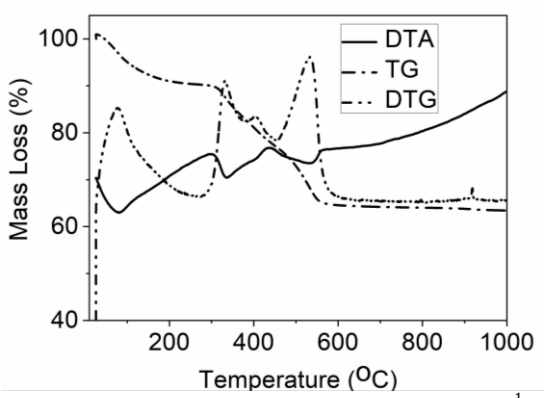

Figure 2: TG/DTA/DTG curves for the $[NiCl_2(L^1)_2]$ complex

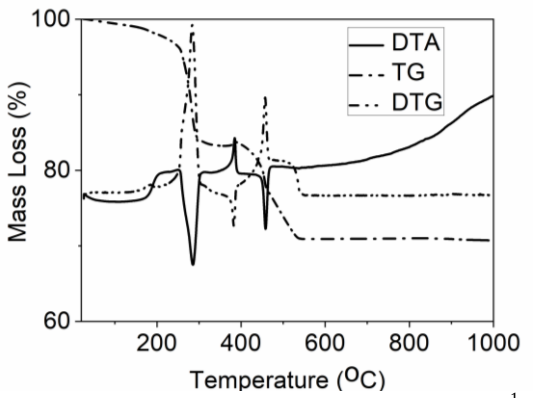

Figure 3: TG/DTA/DTG curves for the $[CuCl_2(L^1)_2]$ complex

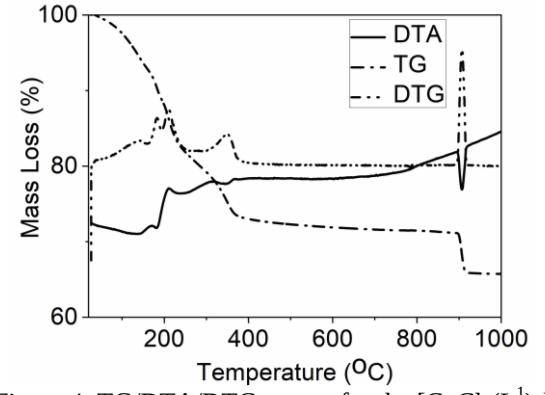

Figure 4: TG/DTA/DTG curves for the $[CoCl_2(L^1)_2]$ complex

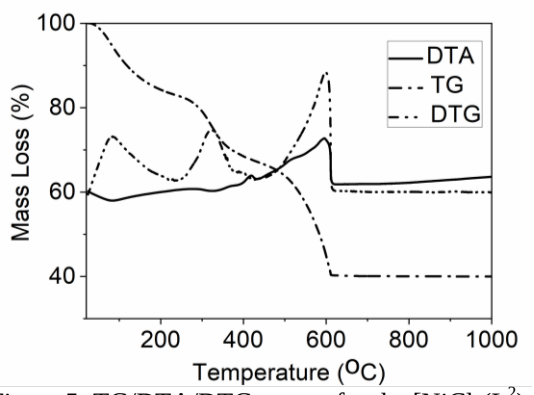

Figure 5: TG/DTA/DTG curves for the $[NiCl_2(L^2)_2]$ complex

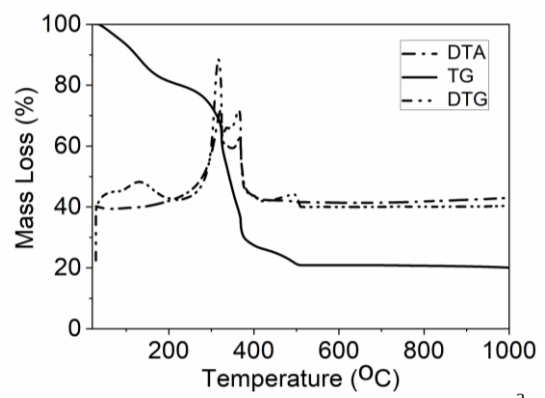

Figure 6: TG/DTA/DTG curves for the $[CuCl_2(L^2)_2]$ complex

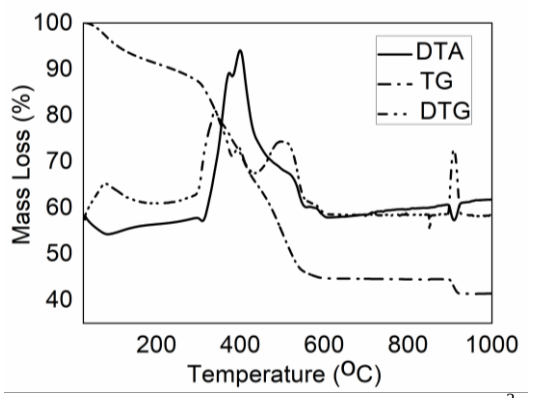

Figure 7: TG/DTA/DTG curves for the$[CoCl_2(L^2)_2]$ complex

The thermal analysis measurements were performed in the temperature range from 25 to 1000 °C, at a heating rate of 10 °C/min under nitrogen gas flow (50 mL/min). The TG/DTA/DTG curves of the complexes are given in Figures 2-7. The DTA curves showed that the complexes decomposed before they reached the melting point, as no melting point was observed. The $[CoCl_2(L^1)_2]$ and $[CuCl_2(L^2)_2]$ complexes decomposed in four steps, while the other complexes decomposed in three steps. After the loss of humidity at 100 °C, the complexes continued to decompose up to 1000 °C. The thermal analysis data are given in Table 2.

The FE-SEM micrographs of the CA/$[ML_2Cl_2]$ hybrid microfibers are given in Figures 8-13. The results showed that the thickness of the CA microfibers was in the range of 4.69-21.25 μm and the thickness of the CA/$[ML_2Cl_2]$ hybrid fibers was less than that of the pristine CA microfibers. This is in line with the findings of other researchers, and it was observed that as the conductivity of the polymer solutions increased the diameter of the fibers decreased.[50] The average fiber thickness of the modified or the hybrid microfibers are given in Table 3.

The EDX spectra of the CA/[ML_2Cl_2] hybrid fibers are given in Figures 14-19. EDX spectra indicate that the metal complexes have been successfully incorporated into the micro/nano-fibers.

Table 2
Thermal analysis data

Complexes	Decomposition steps	TG temperature range, ^oC	Mass loss, %	Residue, %
$[NiCl_2(L^3)_2]$	I	12-221	7.1	64.8
	II	298-362	5.9	
	III	365-738	22.2	
$[CuCl_2(L^3)_2]$	I	15-199	6.8	46.6
	II	244-353	16.9	
	III	456-777	24.8	
	IV	779-931	4.9	
$[CoCl_2(L^3)_2]$	I	10-121	5.5	67.3
	II	132-268	13.5	
	III	279-525	12.8	
	IV	530-611	0.9	
$[NiCl_2(L^4)_2]$	I	175-210	17.5	44.6
	II	210-319	29.6	
	III	431-572	8.3	
$[CuCl_2(L^4)_2]$	I	197-263	34.9	50.7
	II	328-770	11.8	
	III	775-998	2.6	
$[CoCl_2(L^4)_2]$	I	21-194	14	47.9
	II	201-266	8.8	
	III	455-746	29.3	

Table 3
Average fiber thickness of modified microfibers

Composite	Fiber thickness (μm)
CA-$[NiCl_2(L^1)_2]$	1.0-7.0
CA-$[CuCl_2(L^1)_2]$	0.05-4.0
CA-$[CoCl_2(L^1)_2]$	0.05-4.0
CA-$[NiCl_2(L^2)_2]$	0.5-2.5
CA-$[CuCl_2(L^2)_2]$	0.2-7.0
CA-$[CoCl_2(L^2)_2]$	0.5-1.5

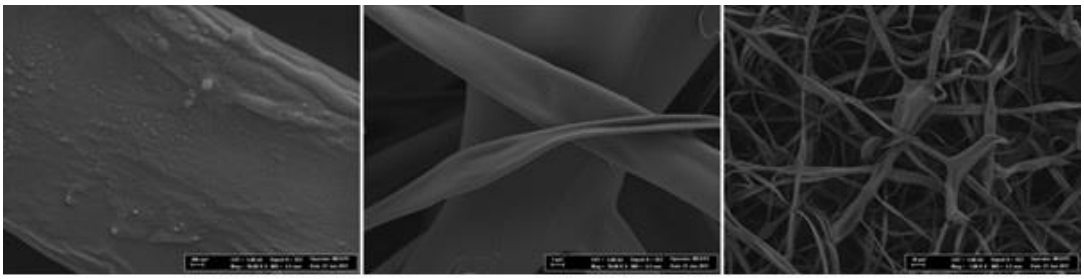

Figure 8: SEM micrographs of CA/$[NiCl_2(L^1)_2]$ hybrid microfibers

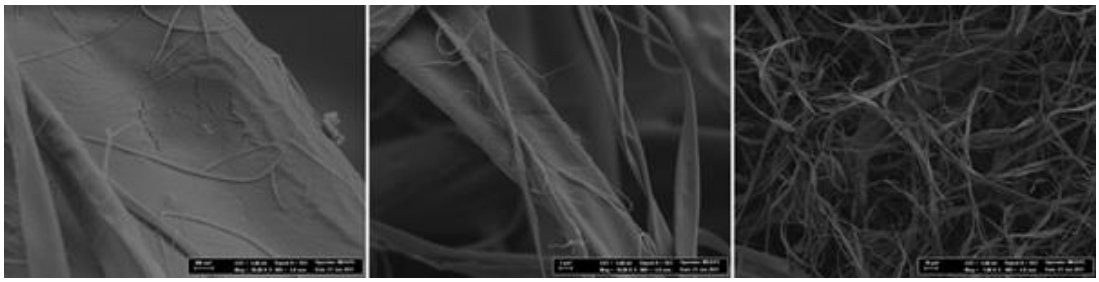

Figure 9: SEM micrographs of CA/[$CuCl_2(L^1)_2$] hybrid microfibers

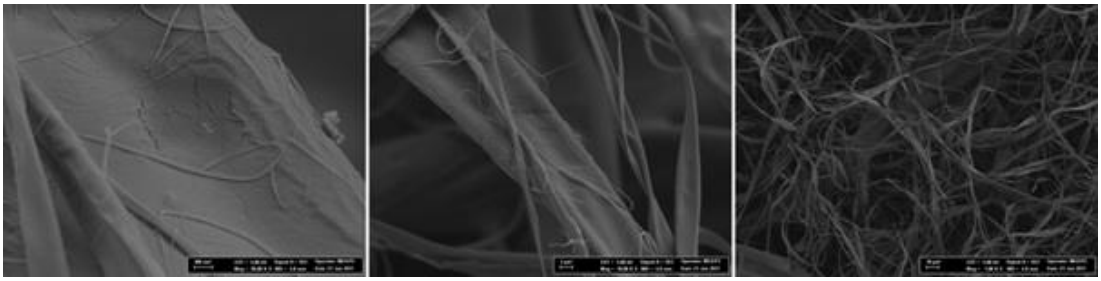

Figure 10: SEM micrographs of CA/[$CoCl_2(L^1)_2$] microfibers

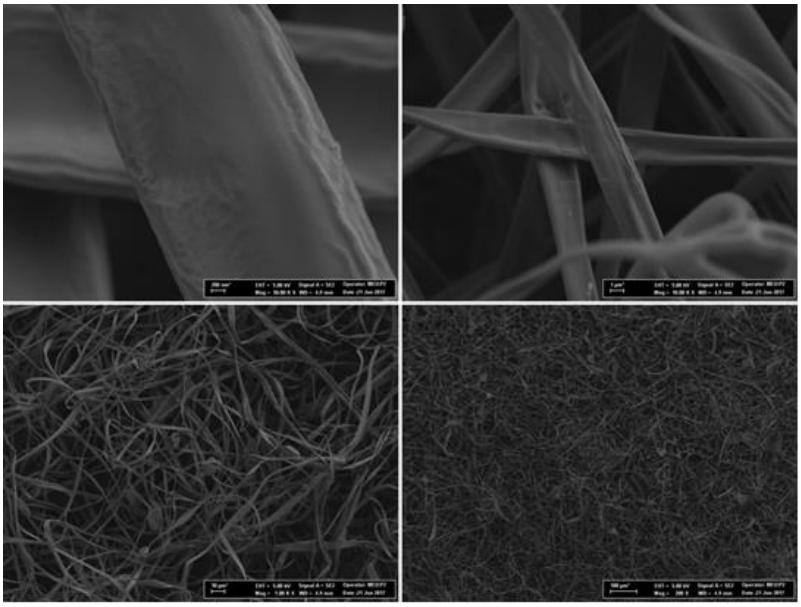

Figure 11: SEM micrographs of CA/[$NiCl_2(L^2)_2$] microfibers

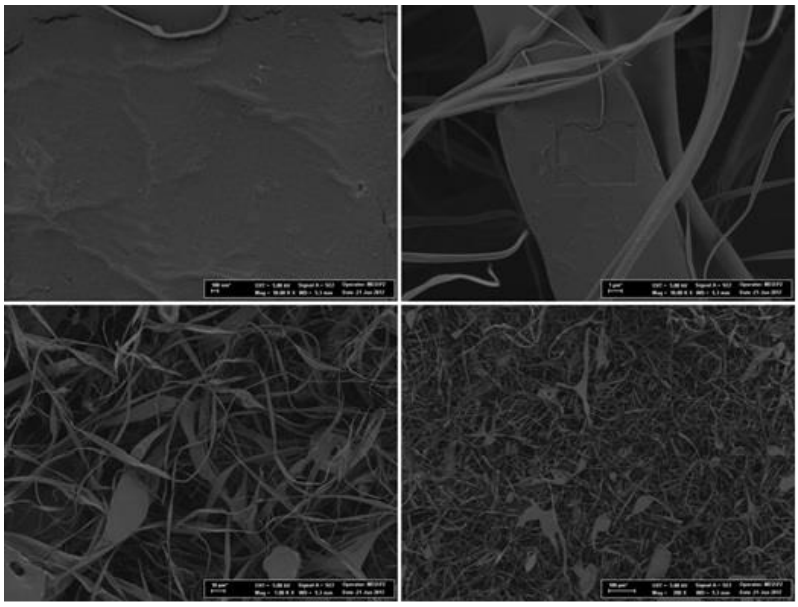

Figure 12: SEM micrographs of CA/[$CuCl_2(L^2)_2$] microfibers

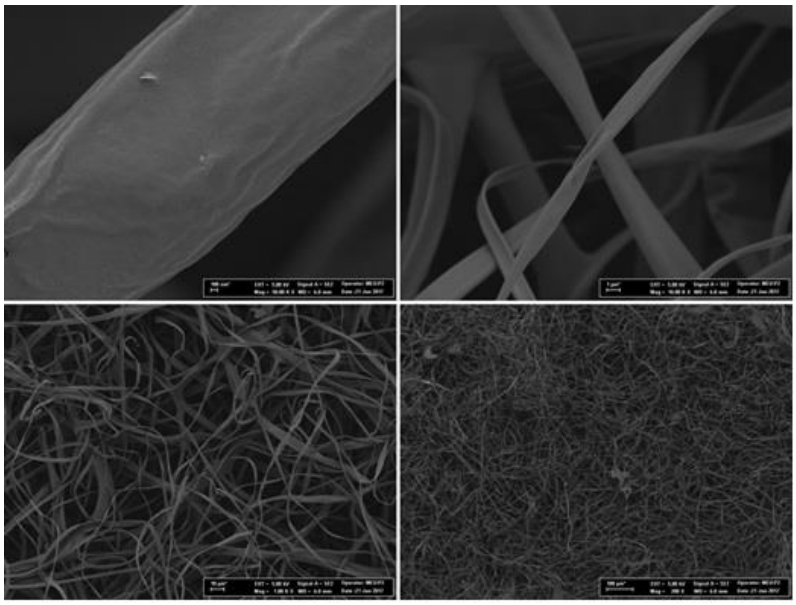

Figure 13: SEM micrographs of CA/[$CoCl_2(L^2)_2$] microfibers

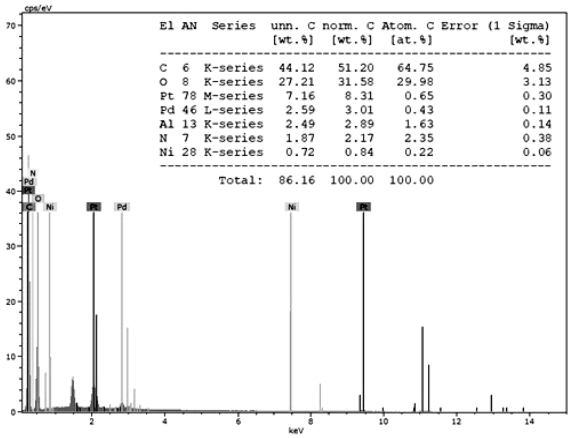

Figure 14: EDX spectra of CA/[$NiCl_2(L^1)_2$] hybrid fibers

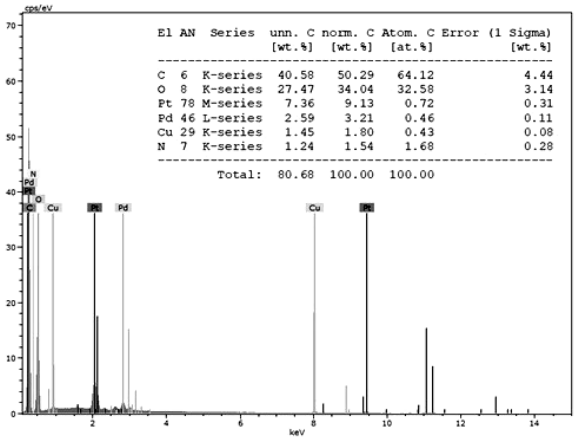

Figure 15: EDX spectra of CA/[$CuCl_2(L^1)_2$] hybrid fibers

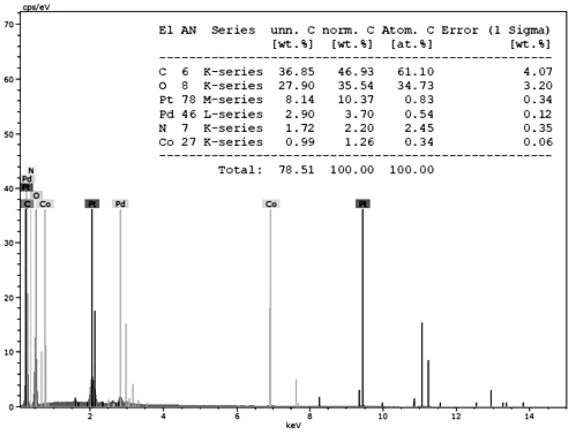

Figure 16: EDX spectra of CA/$[CoCl_2(L^1)_2]$ hybrid fibers

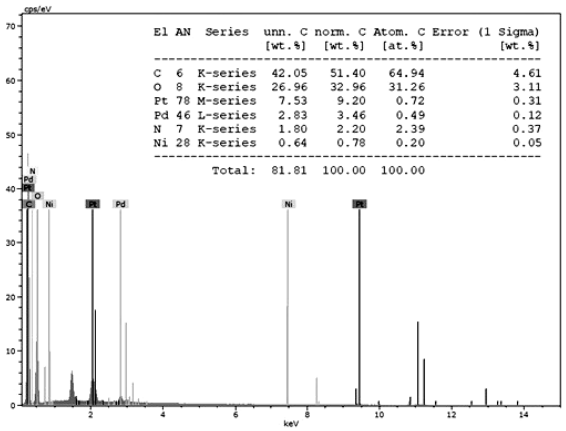

Figure 17: EDX spectra of CA/$[NiCl_2(L^2)_2]$ hybrid fibers

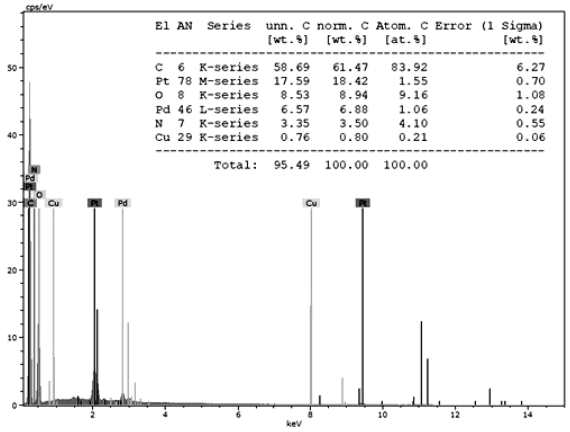

Figure 18: EDX spectra of CA/$[CuCl_2(L^2)_2]$ hybrid fibers

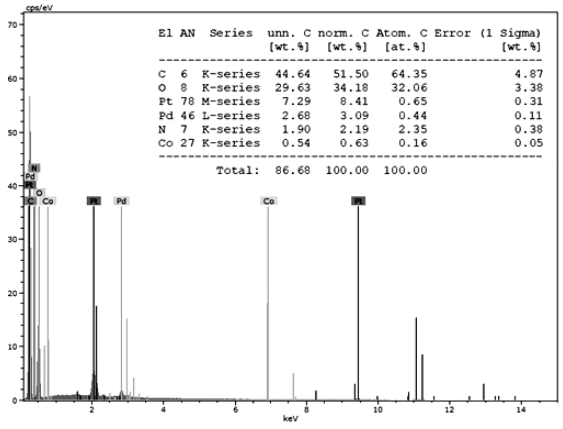

Figure 19: EDX spectra of CA/$[CoCl_2(L^2)_2]$ hybrid fibers

Antibacterial activity studies

The disc diffusion test was performed to investigate the antibacterial activity of the complexes. The inhibition zone diameters obtained and the results of one-way variance analysis (ANOVA) are given in Table 4. According to the data obtained, at a concentration of 3 mg/disc, both the $[NiCl_2(L^1)_2]$ and the $[NiCl_2(L^2)_2]$ complexes were observed to have antibacterial effect against all the bacteria, but the $[CuCl_2(L^2)_2]$ complex did not have antibacterial effect against *K. pneumoniae* nor against *E. faecalis.* As can be seen, the inhibition zone diameter differed for different bacteria, indicating that while some of the bacteria are strongly affected, others are not. The differences in the antibacterial property of the complexes were compared and the differences among the groups were considered meaningful at $p < 0.05$ level. It was observed that the $[CoCl_2(L^1)_2]$ complex formed the largest inhibition zone diameter against MRSA.

The antibacterial properties of all the complexes were compared against the 4 bacterial strains. It was observed that, except for $[CoCl_2(L^2)_2]$, the differences among the groups were meaningful at $p < 0.05$ level. According to these results, the $[CuCl_2(L^1)_2]$, $[CoCl_2(L^1)_2]$ and $[CuCl_2(L^2)_2]$ complexes formed the largest inhibition zone diameter against MRSA.

The minimum inhibitory concentration (MIC) test, or broth microdilution test, was used to determine the effect of the minimum inhibitory concentration of the complexes against the bacteria investigated. According to the results given in Table 5, all the complexes had MIC values in the range from 6.5 $mg.mL^{-1}$ to 0.78 $mg.mL^{-1}$.

Table 4
Growth inhibition zone diameters formed by complexes determined by disk diffusion method (mm)

Test material (complexes) (3 mg/disc)	Antibacterial activity (inhibition zone diameters, mm)			
	**E. coli*	**K. pneumoniae*	***S. aureus*	*E. faecalis*
$[NiCl_2(L^1)_2]$	R	R	R	R
$[CuCl_2(L^1)_2]$	9.0 ± 1.0^{Eb}	9.0 ± 0.6^{Db}	14 ± 1.0^{CDa}	9.0 ± 0.6^{Eb}
$[CoCl_2(L^1)_2]$	15 ± 2.6^{Cab}	12 ± 2.1^{Cab}	16 ± 0.6^{Aa}	11 ± 1.2^{Db}
$[NiCl_2(L^2)_2]$	R	R	R	R
$[CuCl_2(L^2)_2]$	8.0 ± 0.6^{Eb}	R	14 ± 0.6^{BCDa}	R
$[CoCl_2(L^2)_2]$	15 ± 1.5^{BCa}	15 ± 0.6^{Ba}	14 ± 0.6^{BCDa}	14 ± 0.6^{BCa}
Gentamicin (30µg /disc)	24±0.6	22±0.6	21±0.0	20±0.6

Table 5
Minimum reproduction inhibition zone diameters formed by complexes determined by broth microdilution method (mm)

Test material ($[ML_2Cl_2]$ complexes) (50 $mg.mL^{-1}$)	Minimum inhibitory concentration (MIC) value ($mg.mL^{-1}$)			
	**E. coli*	**K. pneumoniae*	***S. aureus*	*E. faecalis*
$[NiCl_2(L^1)_2]$	6.250	6.250	6.250	3.120
$[CuCl_2(L^1)_2]$	3.120	1.560	1.560	1.560
$[CoCl_2(L^1)_2]$	0.780	1.560	0.780	3.120
$[NiCl_2(L^2)_2]$	6.250	6.250	6.250	6.250
$[CuCl_2(L^2)_2]$	6.250	3.120	1.560	3.120
$[CoCl_2(L^2)_2]$	3.120	1.560	1.560	1.560
Gentamicin (0.1 $mg.mL^{-1}$)	0.003	0.003	0.006	0.006

Metal complexes induce the formation of reactive oxygen species (ROS), which are by-products of the metabolism.[51] Due to ROS synthesis, which occurs upon this induction, cell membranes, proteins, DNA and the intracellular system are damaged,[52] and highly reactive radicals that destroy cells are formed.[53] Bis(2-amino-3-methylpyridine)dichloro metal (II) and bis(2,6-diaminopyridine)dichloro metal (II) complexes (metals: Ni(II), Cu(II) and Co(II)) interact with the membrane of the bacteria and induce ROS synthesis and cause oxidative stress of the bacterial membrane, which is lethal for bacterial cells.

Antibacterial activity test results for CA/$[ML_2Cl_2]$ hybrid fibers

The antibacterial activity of the microfibers modified with the complexes was determined according to JIS L 1902:2002. The results regarding the average number of bacteria after 24 h of incubation are given in Table 6, while Table 7 lists the results of the antibacterial activity tests on the fibers. The CA microfibers modified with $[CoCl_2(L^1)_2]$ complexes were determined to have highest activity against *E. coli*, *K. pneumoniae*, *S. aureus* and *E. faecalis.* The hybrid microfibers were observed to have high antibacterial activity, when compared with the antibacterial fabric.

The interaction between the nano/microfiber surfaces and the bacterial membrane is mainly due to the electrostatic interactions in the fiber-bacteria interface and this arises from "contact killing". It was reported that neutralization of the surface charge of bacteria's membrane mediates electrostatic interaction between the membrane and different chemical units.[54,55] Neutralization of the surface charge depends on the balancing interaction between the positively and negatively charged parts of the nano/microfibers and the negatively charged phosphate and carboxylate units on the lipid membranes of the bacteria, and this alters the membrane permeability and thereby causes antimicrobial activity.[55,56]

Table 6
Number of colony forming bacteria (cfb) after incubation on CA/[ML_2Cl_2] hybrid fibers determined by the JIS L 1902 method

Test material	Number of colony formng bacteria (cfb) after incubation			
(CA/[ML_2Cl_2] hybrid fibers)	*_E. coli_	*_K. pneumoniae_	** _S. aureus_	_E. faecalis_
Reproduction control	$3.0x10^7$±1.41	$1.0x10^7$±0.00	$1.0x10^7$±0.00	$8.0x10^6$±4.24
Antibacterial textile	$2.0x10^4$±0.00	$3.0x10^4$±0.70	$1.0x10^4$±0.00	$2.5x10^4$±0.70
CA/[$NiCl_2(L^1)_2$]	$35x10^4$±9.89	$40x10^4$±7.07	$20x10^4$±11.3	$20x10^4$±2.82
CA/[$CuCl_2(L^1)_2$]	$8.0x10^4$±1. 41	$10x10^4$±4.24	$3.5x10^4$±2.12	$8.0x10^4$±2.82
CA/[$CoCl_2(L^1)_2$]	$2.0x10^4$±1.41	$4.0x10^4$±0.70	$1.5x10^4$±0.70	$5.0x10^4$±1.41
CA/[$NiCl_2(L^2)_2$]	$45x10^4$±9.89	$5.0x10^5$±0.70	$40x10^4$±4.24	$15x10^4$±2.82
CA/[$CuCl_2(L^2)_2$]	$7.0x10^4$±5.65	$8.0x10^4$±1.41	$3.0x10^4$±1.41	$9.0x10^4$±0.70
CA/[$CoCl_2(L^2)_2$]	$5.0x10^4$±1.41	$4.5x10^4$±2.12	2.5 $x10^4$±0.70	$3.5x10^4$±0.70
CA/[$NiCl_2(L^3)_2$]	$3.5x10^4$±0.70	$2.5x10^4$±0.70	$3.0x10^4$±1.41	$2.0x10^4$±1.41
CA/[$CuCl_2(L^3)_2$]	$4.0x10^4$±1.41	$4.0x10^4$±0.00	$3.0x10^4$±1.41	$3.5x10^4$±2,12
CA/[$CoCl_2(L^3)_2$]	$2.5x10^4$±0.70	$2.5x10^4$±2.12	$2.0x10^4$±0.00	$2.0x10^4$±0,00
CA/[$NiCl_2(L^4)_2$]	$2.5x10^4$±0.70	$3.0x10^4$±1.41	$2.5x10^4$±2.12	$3.0x10^4$±1.41
CA/[$CuCl_2(L^4)_2$]	$1.5x10^4$±0.70	$1.5x10^4$±0.70	$1.0x10^4$±0.00	$6.5x10^4$±0.70
CA/[$CoCl_2(L^4)_2$]	$1.5x10^4$±2.12	$1.5x10^4$±0.70	$1.0x10^4$±0.00	$1.5x10^4$±0.70

Table 7
Antibacterial activity results for CA/[ML_2Cl_2] hybrid fiber saccording the JIS L 1902 method

Test material	Decrease in reproduction (log cfb)			
(CA/[ML_2Cl_2] hybrid fibers)	*_E. coli_	*_K. pneumoniae_	**_S. aureus_	_E. faecalis_
CA/[$NiCl_2(L^1)_2$]	1.933	1.398	1.699	1.602
CA/[$CuCl_2(L^1)_2$]	2.574	2.000	2.456	2.000
CA/[$CoCl_2(L^1)_2$]	3.176	2.398	2.824	2.205
CA/[$NiCl_2(L^2)_2$]	1.824	2.000	1.398	1.727
CA/[$CuCl_2(L^2)_2$]	2.632	2.097	2.523	1.949
CA/[$CoCl_2(L^2)_2$]	2.477	2.347	2.603	2.359
CA/[$NiCl_2(L^3)_2$]	2.933	2.603	2.523	2.602
CA/[$CuCl_2(L^3)_2$]	2.875	3.000	2.523	2.359
CA/[$CoCl_2(L^3)_2$]	3.080	2.603	2.699	2.602
CA/[$NiCl_2(L^4)_2$]	3.080	2.523	2.603	2.426
CA/[$CuCl_2(L^4)_2$]	3.301	2.824	3.000	2.091
CA/[$CoCl_2(L^4)_2$]	3.301	2.824	3.000	2.727

The contact between the hybrid nano/microfibers obtained via modification of the polymer matrix with the metal complexes and the bacterial membrane takes place not only through the charged groups on the polymer surface, but also through the metal complexes incorporated into the fibers. This may also be due to the possible ROS synthesis arising from the interaction of the complexes with the bacteria upon their diffusion through the pores of the hybrid nano/microfibers. Another possible reason for this may be the effect that the interaction between the partially negative electron clouds of the ligands in the metal complexes in the nano/microfibers and the partially positive charge distribution of the central metal cation exerts on the bacteria membrane. The hybrid nano/microfibers were observed to affect both the gram-positive and the gram-negative bacteria.

CONCLUSION

In this study, complexes with the general formula [ML_2Cl_2] (L: 2-amino-3-methylpyridine, 2,6-diamino pyridine; M: Ni (II), Cu(II), Co(II)) were synthesized and their structures were elucidated via FT-IR, ^{1}H-NMR and ^{13}C-NMR techniques. The thus-prepared complexes were used to functionalize a cellulose-based biocompatible, biodegradable, eco-friendly polymer – cellulose acetate (CA). The CA/[ML_2Cl_2] hybrid microfibers were obtained via a robust, eco-friendly and green method – electrospinning. The morphologies and the mean diameters of the fibers were determined from the FE-SEM images of the electrospun hybrid microfibers, and their structures were elucidated by using their FT-IR and XRD spectra. The thermal properties of the synthesized complexes were investigated by

using the data obtained in the TG/DTA/DTG analyses. The FT-IR spectra of CA microfibers containing pyridine-derived complexes are similar to those of pure CA fibers.

The antibacterial activity of the pyridine complexes against extended spectrum beta-lactamase producing gram-negative (*Escherichia coli* and *Klebsiella pneumonia*) and gram-positive (methicillin-resistant *Staphylococcus aureus* and *Enterococcus faecalis*) bacterial strains was investigated by the modified disc diffusion test (CLSI-M02-A11) and the broth microdilution method (CLSI-M07-A9), while the antibacterial activity of the CA/[ML_2Cl_2] hybrid microfibers was determined according to the JIS L 1902: 2008 Testing method for antibacterial activity of textiles. The amount of the complexes to be used in producing the functionalized fibers was determined via the minimal inhibitory concentration (MIC) test, as this test provides both bacteriostatic and bactericidal results, besides allowing sufficient time for the bacteria to grow on a given antimicrobial fabric. The quantitative methods – JIS L 1902:2008 – allowed determining the exact value of the antimicrobial activity, which was performed by calculating the reduction in bacterial growth against a control. According to the results obtained in three different ways, all the complexes and the prepared fiber mats containing these complexes were found to have antibacterial activity. However, it was found out that MRSA was more sensitive than *E. coli*.

The results showed that the hybrid microfibers obtained by modifying the CA/HPMC copolymer with the complexes are effective against hospital microbes and these microfibers can be used in the production of disposable hospital textiles, which would be of great value, especially in intervention in the case of infections, providing relief to health care systems and to patients, especially in epidemics, such as SARS, MERS and COVID-19.

ACKNOWLEDGEMENTS: This study was supported by TUBİTAK under Project number 116Z295, Çankırı Karatekin University BAP under Project number FF060416B23 and Burdur Mehmet Akif Ersoy University BAP under Project number 0432-YL-17. The author also would like to thank Prof. Dr. Fatih Mehmet EMEN, Assoc. Prof. Dr. Şinasi AŞKAR, Assoc. Prof. Dr. Tuncay YEŞİLKAYNAK and Assist. Prof. Dr. Zehra ALTIN for their valuable contribution.

REFERENCES

[1] WHO, Global Action Plan on Antimicrobial Resistance, (2015), https://www.who.int/publications/i/item/9789241509763

[2] C. Kirchhelle, A. Roberts and A. C. Singer, *Sci. Am.*, (2020), https://blogs.scientificamerican.com/observations/antibiotic-resistance-could-lead-to-more-covid-19-deaths/

[3] C. Huang, Y. Wang, X. Li, L. Ren, J. Zhao *et al*., *Lancet*, **395**, 497 (2020), https://doi.org/10.1016/S0140-6736(20)30183-5

[4] X. Li, L. Wang, S. Yan, F. Yang, L. Xiang *et al*., *Int. J. Infect. Dis.*, **94**, 128 (2020), https://doi.org/10.1016/j.ijid.2020.03.053

[5] F. Yap, *Crit. Care*, **8**, 220 (2004), https://doi.org/10.1186/cc2687

[6] J. Louie, C. Jean, T. H. Chen, S. Park, R. Ueki *et al*., *Morb. Mortal. Wkly Rep*., **58**, 1071 (2009), http://www.cdc.gov/.../mm5838.pdf

[7] F. Zhou, T. Yu, R. Du, G. Fan, Y. Liu *et al*., *Lancet*, **395**, 1014 (2020), https://doi.org/10.1016/S0140-6736(20)30566-3

[8] A. Filia, A. Bella, M. Del Manso, M. Baggieri, F. Magurano *et al*., *Eur. Surveil*., **22** (2017), http://dx.doi.org/10.2807/1560-7917.ES.2017.22.37.30614

[9] J. Cao, W. J. Tu, W. Cheng, L. Yu, Y. K. Liu *et al*., *Clin. Infect. Dis*., **71**, 748 (2020), https://doi.org/10.1093/cid/ciaa243

[10] H. F. L. Wertheim, D. C. Melles, M. C. Vos, W. Van Leeuwen, A. Van Belkum *et al*., *Lancet Infect. Dis*., **5**, 751 (2005), https://doi.org/10.1016/S1473-3099(05)70295-4

[11] J. Kluytmans, A. Van Belkum and H. Verbrugh, *Clin. Microbiol. Rev*., **10**, 505 (1997), https://doi.org/10.1128/CMR.10.3.505

[12] T. Lupia, S. Scabini, S. M. Pinna, G. Di Perri, F. G. De Rosa *et al*., *J. Glob. Antimicrob. Resist*., **21**, 22 (2020), https://doi.org/10.1016/j.jgar.2020.02.021

[13] Z. Wang, B. Yang, Q. Li, L. Wen and R. Zhang, *Clin. Infect. Dis*., **71**, 769 (2020), https://doi.org/10.1093/cid/ciaa272

[14] L. Wang, W. He, X. Yu, D. Hu, M. Bao *et al*., *J. Infect*., **80**, 639 (2020), https://doi.org/10.1016/j.jinf.2020.03.019

[15] L. K. Landeen, M. T. Yahya and C. P. Gerba, *Appl. Environ. Microbiol*., **55**, 3045 (1989),

https://doi.org/10.1128/aem.55.12.3045-3050.1989
[16] B. H. Pyle, S. C. Broadaway and G. A. McFeters, *J. Appl. Bacteriol.*, **72**, 71 (1992), https://doi.org/10.1128/AEM.65.5.1966-1972.1999
[17] R. D. Scott, S. L. Solomon and J. E. McGowan, *Emerg. Infect. Dis.*, **7**, 282 (2001), https://doi.org/10.3201/eid0702.010227
[18] WHO Guidelines on Prevention and Control of Hospital Associated Infections (2002), https://apps.who.int/iris/bitstream/handle/10665/205187/B0007.pdf?sequence=1&isAllowed=y
[19] Y. Y. Zhang, Q. B. Xu, F. Fu and X. D. Liu, *Cellulose*, **23**, 2791 (2016), https://doi.org/10.1007/s10570-016-1012-0
[20] A. Muñoz-Bonilla, C. Echeverria, Á. Sonseca, M. P. Arrieta and M. Fernández-García, *Materials*, **12**, 1312 (2019), https://doi.org/10.3390/ma12081312
[21] R. E. Demirdogen, T. Yeşilkaynak, T. Tishakova and F. M. Emen, *Chem. Chem. Technol.*, **15**, 217 (2021), https://doi.org/10.23939/chcht15.02.217
[22] R. R. Watkins and R. A. Bonomo, *Expert. Rev. Anti. Infect. Ther.*, **11**, 543 (2013), https://doi.org/10.1586/eri.13.46
[23] K. Y. Djoko, E. Maud, S. Achard, M. D. Phan, A. W. Lo *et al.*, *Antimicrob. Agents Chemother.*, **62**, 2 (2018), https://doi.org/10.1128/AAC.02280-17
[24] H. Shaghaleh, X. Xu and S. Wang, *RSC Adv.*, **8**, 825 (2018), https://doi.org/10.1039/C7RA11157F
[25] J. Shokri and K. Adibki, *Pharm. Elect. Appl.*, (2013), http://dx.doi.org/10.5772/55178
[26] J. S. Novais, M. F. Carvalho, M. S. Ramundo, C. O. Beltrame, R. B. Geraldo *et al.*, *Sci. Rep.*, **10**, 1 (2020), https://doi.org/10.1038/s41598-020-76372-z
[27] T. Suksrichavalit, S. Prachayasittikul, C. Nantasenamat, C. Isarankura-Na-Ayudhya and V. Prachayasittikul, *Eur. J. Med. Chem.*, **44**, 3259 (2009), https://doi.org/10.1016/j.ejmech.2009.03.033
[28] Z. Ma, F. E. Jacobsen and D. P. Giedroc, *Chem. Rev.*, **109**, 4644 (2009), https://doi.org/10.1021/cr900077w
[29] K. L. Haas and K. J. Franz, *Chem. Rev.*, **109**, 4921 (2009), https://doi.org/10.1021/cr900134a
[30] M. Okamoto, K. I. Takahashi, T. Doi and Y. Takimoto, *Anal. Chem.*, **69**, 2919 (1997), https://doi.org/10.1021/ac960910s
[31] Z. Dega-Szafran, A. Kania, B. Nowak-Wydra and M. Szafran, *J. Mol. Struct.*, **322**, 223 (1994), https://doi.org/10.1016/0022-2860(94)87039-X
[32] P. Carmona and M. Molina, *Spectrochim. Acta*, **49A**, 1 (1993), https://doi.org/10.1016/0584-8539(93)80255-9
[33] R. E. Demirdogen, D. Kilic, F. M. Emen, Ş. Aşkar, A. İ. Karaçolak *et al.*, *J. Mol. Struct.*, **1204**, 127537 (2020), https://doi.org/10.1016/j.molstruc.2019.127537
[34] K. J. Waldron and N. J. Robinson, *Nat. Rev. Microbiol.*, **7**, 25 (2009), https://doi.org/10.1038/nrmicro2057
[35] K. Joyce, S. Saxena, A. Williams, C. Damurjian, N. Auricchio *et al.*, *J. Antibiot.*, **63**, 530 (2010), https://doi.org/10.1038/ja.2010.64
[36] S. A. Wilks, H. Michels and C. W. Keevil, *Int. J. Food Microbiol.*, **105**, 445 (2005), https://doi.org/10.1016/j.ijfoodmicro.2005.04.021
[37] C. Espírito Santo, E. W. Lam, C. G. Elowsky, D. Quaranta, D. W. Domaille *et al.*, *Appl. Environ. Microbiol.*, **77**, 794 (2011), https://doi.org/10.1002/mbo3.2
[38] D. Quaranta, T. Krans, C. Espírito Santo, C. G. Elowsky, D. W. Domaille *et al.*, *Appl. Environ. Microbiol.*, **77**, 416 (2011), https://doi.org/10.1128/AEM.01704-10
[39] N. Behera, M. Arakha, M. Priyadarshinee, B. S. Pattanayak, S. Soren *et al.*, *RSC Adv.*, **9**, 24888 (2019), https://doi.org/10.1039/C9RA02082A
[40] G. Satpathy and E. Manikandan, *Int. J. Eng. Adv. Technol.*, **8**, 3684 (2019), https://doi.org/10.35940/ijeat.F9374.088619
[41] S. L. Warnes, V. Caves and C. W. Keevil, *Environ. Microbiol.*, **14**, 1730 (2012), https://doi.org/10.1111/j.1462-2920.2011.02677.x
[42] R. Hong, T. Y. Kang, C. A. Michels and N. Gadura, *Appl. Environ. Microbiol.*, **78**, 1776 (2012), https://doi.org/10.1128/AEM.07068-11
[43] J. R. Allan, D. H. Brown, R. H. Nuttall and D. W. A. Sharp, *J. Inorg. Nucl. Chem.*, **27**, 1529 (1965), https://doi.org/10.1016/0022-1902(65)80014-8
[44] C. Wiegand, M. Abel, P. Ruth, P. Elsner and U. C. Hipler, *J. Mater. Sci.: Mater. Med.*, **26**, 18 (2015), https://doi.org/10.1007/s10856-014-5343-9
[45] N. Sundaraganesan, S. Ilakiamani, B. Anand, H. Saleem and B. D. Joshua, *Spectrochim. Acta A*, **64**, 586 (2006), https://doi.org/10.1016/j.saa.2005.07.061
[46] J. F. Arenas, I. López Tocón, J. C. Otero and J. I. Marcos, *J. Mol. Struct.*, **410**, 443 (1997), https://doi.org/10.1016/S0022-2860(96)09699-8
[47] J. Karpagam, N. Sundaraganesan, S. Kalaichelvan and S. Sebastian, *Spectrochim. Acta A*, **76**, 502 (2010), https://doi.org/10.1016/j.saa.2010.04.013

[48] N. Sundaraganesan, C. Meganathan and M. Kurt, *J. Mol. Struct*., **891**, 284 (2008), https://doi.org/10.1016/j.molstruc.2008.03.051
[49] M. S. Peresin, Y. Habibi, A. H. Vesterinen, O. J. Rojas, J. J. Pawlak *et al*., *Biomacromolecules*, **11**, 2471 (2010), https://doi.org/10.1021/bm901254n
[50] W. Lin, Y. W. Huang, X. D. Zhou and Y. Ma, *Int. J. Toxicol*., **25**, 451 (2006), https://doi.org/10.1080/10915810600959543
[51] X. H.Vu, T. T. T. Duong, T. T. H. Pham, D. K. Trinh, X. H. Nguyen *et al*., *Adv. Nat. Sci*.: *Nanosci. Nanotechnol*., **9**, 025019 (2018), https://doi.org/10.1088/2043-6254/aac58f
[52] J. S. Kim, E. Kuk, K. N. Yu, J. H. Kim, S. J. Park *et al*., *Biol. Med*., **3**, 95 (2007), https://doi.org/10.1016/j.nano.2006.12.001
[53] M. Arakha, S. Pal, D. Samantarrai, T. K. Panigrahi, B. C. Mallick *et al*., *Sci. Rep*., **5**, 1 (2015), https://doi.org/10.1038/srep14813
[54] S. Halder, K. K. Yadav, R. Sarkar, S. Mukherjee, P. Saha *et al*., *SpringerPlus*, **4**, 1 (2015), https://doi.org/10.1186/s40064-015-1476-7
[55] C. S. Alves, M. N. Melo, H. G. Franquelim, R. Ferre, M. Planas *et al*., *J. Biol. Chem*., **28**5, 27536 (2010), https://doi.org/10.1074/jbc.M110.130955